POLITECNICO DI TORINO
Repository ISTITUZIONALE

Kraft Lignin Modification and Application as Aqueous Binder for Carbon Anode in Lithium Battery

Original
Kraft Lignin Modification and Application as Aqueous Binder for Carbon Anode in Lithium Battery / Izaguirre, N., Lingua, G., Piovano, A., Gerbaldi, C., Mecerreyes, D., Labidi, J.. - In: ACS APPLIED POLYMER MATERIALS. - ISSN 2637-6105. - STAMPA. - 7:6(2025), pp. 3764-3773. [10.1021/acsapm.4c04099]

Availability:
This version is available at: 11583/2998651 since: 2025-03-29T20:39:30Z

Publisher:
American Chemical Society

Published
DOI:10.1021/acsapm.4c04099

Terms of use:

This article is made available under terms and conditions as specified in the corresponding bibliographic description in the repository

Publisher copyright
ACS postprint/Author's Accepted Manuscript

This document is the Accepted Manuscript version of a Published Work that appeared in final form in ACS APPLIED POLYMER MATERIALS, copyright © American Chemical Society after peer review and technical editing by the publisher. To access the final edited and published work see http://dx.doi.org/10.1021/acsapm.4c04099.

(Article begins on next page)

19 November 2026

Kraft Lignin Valorization Through Chemical Modification and Application as a Binder Material in Lithium Battery Electrodes

Nagore Izaguirre[a], Gabriele Lingua[b*], Alessandro Piovano[c], Claudio Gerbaldi[c], David Mecerreyes[b,d] and Jalel Labidi[a*]

[a] Biorefinery Processes Research Group, Chemical and Environmental Engineering Department, Engineering Faculty of Gipuzkoa, University of the Basque Country UPV/EHU, Plaza Europa 1, 20018 Donostia, Spain.

[b] POLYMAT University of the Basque country UPV/EHU, Avenida Tolosa, 72, 2008, Donostia-San Sebastian, Spain

[c] GAME Lab, Department of Applied Science and Technology (DISAT), Politecnico di Torino, C.so Duca Degli Abruzzi 24, 10129, Torino, Italy

[d] IKERBASQUE, Basque Foundation for Science, 48009, Bilbao, Spain

*Corresponding authors: gabriele.lingua@polymat.eu, jalel.labidi@ehu.eus

Abstract

Although lithium batteries contribute to a green energy economy most of the materials used in their production are fossil-based. A way to diminish the carbon footprint is by utilizing sustainable and biobased products like lignin, which is highly abundant in nature and vastly produced industrially as a low-value side product in the paper and pulp industry. In the current work, chemically modified Kraft lignins (KL) with different chemical functionalities such as carboxymethyl and sulfomethyl were applied as binder materials for preparing active carbon-based electrodes for lithium metal lab-scale battery cells. The optimization of the lignin binders through functionalization allowed for a significantly enhanced aqueous processability and performance of anodic electrodes composed of hard carbon as the electroactive material, and carbon black as the conducting additive. Battery performances were comparable with the state-of-the-art biopolymer binders carboxymethylcellulose (CMC) reaching specific capacity values of 170 mA h/g. The functionalization shows an alternative approach to the valorization of lignin in high-tech applications.

Keywords: Aqueous binders, Lignin-based polymers, Batteries, Green chemistry, Biopolymers

INTRODUCTION

Lithium batteries, comprising primary Lithium-metal (LMBs) and rechargeable Lithium-ion (LIBs), are considered to be crucial in the transition to a more sustainable energy economy [1]. Especially considering the development of the renewable energy, it is now essential having energy storage devices to satisfy the power needs of storing a fair amount of energy [2–4]. However, current lithium batteries imply the use of advanced and scarce materials and technologies, increasing the cost of these devices and creating an urge to find solutions for material depletion. One approach to promote a global sustainable transition in manufacturing these devices would be based on the implementation of bio-based materials [5]. Lignin is the second most abundant biopolymer on earth, and it is underutilized as a low-value side product in the paper and pulp industry despite its complex and highly aromatic structure with interesting properties [6]. Approximately 70 million tons of lignin are generated from industrial cellulose pulping processes, from which less than 2 wt. % is utilized in products like additives, stabilizers, dispersants, and surfactants [7–9]. This underutilization sparks the desire to develop not only processes to isolate lignin from biomass more efficiently, but also to engineer lignin-based products for energy storage devices to increase the commercial value. Indeed, Lignin and carboxymethylcellulose (CMC) are both biopolymers derived from plant materials, but they differ significantly in terms of production processes and sustainability [10].

Generally, battery electrodes are composed of active material, a conductive agent or additive, and a binder material, which greatly influence the properties of the final battery. Although the binder is the electrochemically inactive component of the electrode, it has a key role in the overall performance, being responsible for the electrode integrity and affecting electrochemical processes [11]. The binder materials are usually polymeric compounds with the main role of holding together the inorganic powders (active material and conductive agent) in a continuous network, providing at the same time a stable and efficient contact with the metal current collector [12]. Binder materials can be divided into two main categories: the ones that are used in the processing of electrodes using organic solvents and the ones that are used for water processing. The solubility of the binders is fundamental for the electrode preparation since the proper mixing of the powders with the polymer chains is achieved by dispersing the powders into a polymer solution, and then this slurry is casted onto the metal current collector. Polyvinilidene fluoride (PVDF) is nowadays the commercially dominating binder material, and belongs to the first category [13]. Other polymers like styrene butadiene rubber (SBR) [14], carboxymethylcellulose (CMC) [15] in

combination with different latexes including bio-based ones, and acrylonitrile based polymers (PAN) are recently proposed as promising binders for aqueous processing [16].

Polyvinylidene fluoride (PVDF) is widely used along the N-methyl-2-pyrrolidone (NMP) solvent in electrode formulation. The European Union regulatory system has considered these fluorinated substances of high concern, suggesting the development of more environmentally friendly alternatives [17]. Water is the solvent that has attracted intensive interest in research, due to its economic and environmental benefits [18], that combined with the appropriate source of raw materials and the substitution of the currently used scarce materials for alternative materials [19] would reduce both the social and the environmental impact associated with the battery manufacturing process [20–23]. Among the current aqueous binders, CMC is the most popular one, produced by adding carboxymethyl side-groups into cellulose, a linear polymer made up of polysaccharides. This way, the molecules have amphiphilic properties, where the hydrophilic part (the carboxymethyl groups) interacts with water while the hydrophobic one (the cellulose backbone chain) adheres to the carbon particles enveloping them, increasing the stability due to the steric effect and electrostatic repulsion [24]. Moreover, CMC and SBR latex combinations have also been widely employed as multi-component polymer binders for LIBs. SBR has higher binding forces and is a more flexible elastomer, bringing higher tensile ratio, cyclability, and mechanical stability to the cell [14,25]. Other gums, carrageenans, and alginate are among the most typical biomass-derived natural binders too. Their unique functionality, environmental friendliness, sustainability, and low price convert them into potential candidates for developing “green battery” systems with high performance [26–31]. For instance, carrageenans are biobased sulfonated polysaccharides that have been studied as binder for high-voltage NMC cathodes [32]. Alternatively, biobased acrylic latexes have been combined with CMC for enhanced adhesion and flexibility [33].

Lignin is the most abundant aromatic biopolymer on Earth, since it is a main component in all lignocellulosic biomass. It provides rigidity and strength to plant tissues, controls the fluid flow, and protects plants from biochemical stress [34]. Lignin is a three-dimensional polymer composed of three different units, p-hydrophenyl (H), syringyl (S), and guiacyl (G), which are interconnected by different bonds and randomly polymerized by radical reactions without any specific order. Depending on the extraction process carried out, and other factors like biomass source and climatic conditions, its physicochemical properties can significantly differ, complicating the large-scale processing [35]. The sulfite and Kraft methods are the two main industrial lignin extraction processes, based on alkaline delignification. The first one employs sulfite (SO_3^{2-}) or bisulfite (HSO_3^-) salts, obtaining

lignosulfonates, which are particularly interesting due to the high degree of solubility in water [36]. However, the high degradation rate and high sulfur content, as well as the drastic decrease in the market share, make it an uncertain prospect to use as feedstock [37]. On the other side, the Kraft method is the most used on the industrial scale, with a share of 90% of the total pulp production [38]. It is carried out in a NaOH and Na_2S aqueous solution, where HS^- ions present in the medium enhance the delignification process, obtaining high-quality pulp. The lignin obtained has a high molecular weight, but unlike the lignosulfonates, is hydrophobic [39]. Nevertheless, this type of pulping has increased by 150% from 2014 to 2018, with an additional market pull expectancy [38]. Its phenolic structure and quinone groups are redox active sites present in lignin, which favor lithium-ion transport and electrolyte affinity. Moreover, its overall structure gives hardness and resistance to heat and chemicals [40]. Lignin has been reported as binder material without carrying out any treatment [41], preparing a mixture with silicium particles [42], or by modifying it with aminoacids for Li-S batteries [43]. Nevertheless, the majority of the works about the application of lignin into battery electrodes has concerned its use as active material through carbonization [44].

Nevertheless, due to the heterogeneous structure of the obtained lignin, the process needs to be optimized. This optimization also involves the functionalization of the lignin to achieve specific features that directly influence the performance of the composite electrode.

In this work we investigated the optimization of lignin as a binder for anodic electrodes for lithium batteries, analyzing the effect of different lignin functionalization on the performance and stability of the battery cells. To do this, two different functionalization processes were carried out to prepare carboxymethylated Kraft lignin (CMKL) and sulfomethylated Kraft lignin (SMKL) with highly polar groups that not only improve the processability in water but also strongly interact with lithium ions. The functional lignins were fully characterized from the physicochemical and thermal viewpoints (FTIR, GPC, NMR, TGA, and DSC) and used in electrodes in combination with the active carbon (AC) and conducting additive (CA), in a AC:CA:Binder ratio of 92:3:5. The electrochemical results obtained using the functionalized lignin were compared with other commonly used binders to evaluate the valorization possibilities for the lignin in lithium batteries.

MATERIALS AND METHODS

Materials

KL was obtained from the Kraft liquor supplied by a local paper and pulp industry (Papelera Zikuñaga). The lignin was precipitated from the liquor adding concentrated H_2SO_4 (96 % technical grade, PanReac). The carboxymethylation reaction was carried out employing NaOH (PanReac) and sodium chloroacetate (SCA) (Sigma), while for the sulfomethylation, apart from the same NaOH, formaldehyde (37 %, Panreac) and sodium sulfate (Na_2SO_4) (Sigma) were employed.

For the electrodes preparation and the Li metal cells assembly (CR2032-coin cell), the used materials were active carbon (AC, Biohard Carbon (HC) Type 2 (5 μm)), Copper foils, Carbon black C45 (Timcal), Lithium metal foils (Gelon energy, 100 μm thick), 1 M $LiPF_6$ in Ethylene carbonate:Diethyl carbonate (EC:DEC) 1:1 v/v (Solvionic) and Whatman® glass microfiber grade GF/B separators were used. Fiberglass separators were vacuum dried at 110 °C for 48h before use.

Physicochemical characterization

Gel Permeation Chromatography (GPC) was used to calculate the weight average molecular weight (M_w). A Jasco LC-Net II/ADC device with a RI-2031 Plus Intelligent refractive index detector, two PolarGel-M columns (300 mm × 7.5 mm) placed in series, and a PolarGel-M guard (50 mm × 7.5 mm) was used. 20 μL of 50 ppm lignin solution was injected for each measurement and eluded the mobile phase (DMF with 0.1 % LiBr) at 40 °C and 0.7 mL/min flow rate. The calibration curve was obtained with polystyrene standards of molecular weights ranging from 266 to 70,000 g/mol.

^{13}C NMR spectroscopy was used to determine the structural features of the KL, CMKL, and SMKL. The samples were diluted in DMSO-d_6 and 100 mg/mL solutions were prepared. The spectra were recorded in a Bruker AVANCE 500 MHz. Some specific ranges of the spectra obtained were integrated for a semiquantitative determination of the abundance of different types of carbon atoms present in the modified lignins.

^{31}P NMR spectra were recorded similarly in a Bruker AVANCE 500 MHz, and a quantitative procedure was followed to determine the concentrations of different hydroxyl groups present in lignin. For that, 50 mg of lignin sample were dissolved in a Pyridine (Py) and deuterated chloroform ($CDCl_3$) solvent mixture in a ratio of 1.6:1 (v/v), and 0.1 mL of internal standard (IS) solution composed by 5 mg/mL of Chromium(III) acetylacetonate ($Cr(acac)_3$) and 18 mg/mL of endo-N-hydroxy-5-norbornene-2,3-dicarboximide (NHND) dissolved in the same Py and $CDCl_3$ solvent mixture. Once the solution was fully dissolved

2-Chloro-4,4,5,5-tetramethyl-1,3.2-dioxaphospholane (TMDP) was added to react with all the hydroxyl groups in the sample and showed the signal in the ^{31}P NMR spectra. The signal attributed to NHND at 151 ppm is integrated first and used as a reference to calculate the concentration of the different phenolic OH groups present in lignin at the signal range of 144-137 ppm (syringyl (S) at 144-141.5 ppm, guaiacyl (G) at 140.5-139 ppm, and p-hydroxyphenyl (H)) at 139-137 ppm), aliphatic OH groups at 150-145 ppm, and carboxylic acid OH groups at 136-134 ppm.

Thermogravimetric analyses were performed using a Mettler Toledo TGA 851 with a heating circulator type F32-HL from Julabo GmbH. 70 µL alumina crucibles were used to store around 5 mg of sample, which were heated from 25 to 800 °C at a 10 °C/min heating rate under inert conditions (Ar), in a 40 mL/min flow rate.

Differential Scanning Calorimetry was performed using a DSC822e (Mettler Toledo). The process consisted of heating from 25–225 °C at 10 °C/min, followed by cooling to 25 °C at the same rate. Finally, a second heating to 225 °C was performed with the same parameters as the first one. This scan was used to determine the glass transition temperature (T_g) of each sample.

A solubility and swelling test were also conducted to determine the interactions happening with the selected electrolyte for the cell configuration. Therefore, 1g of binder material previously pressure-pressed was submerged in the electrolyte for 1 day. After this time the binder materials were retrieved from the electrolyte, dried, and weighed.

Electrochemical characterization

KL, CMKL, and SMKL were employed as binder material for the preparation of negative electrodes for Li metal cells and the device performance were compared with the one using a widely employed commercial biomaterial such as CMC binder.

The formulation used for the preparation of all the electrodes was the following: 92% AC (Biohard Carbon (HC) Type 2 (5 m)), 3% CA (Carbon Black C45, since the solvent used for the slurry preparation was deionized water), and 5% of binder. The slurry was homogenized using an automatic mixer (FlackTek speedmixer, DAC 330-100 SE). The conditions were set at 3000 rpm for 3 minutes, and the process was repeated twice, until a homogeneous 5 wt. % concentration slurry mixture was obtained.

Once a homogeneous slurry was obtained, the electrodes were prepared using an automatic doctor-blade machine. Cu foil was used as the current collector, and the slurry was spread with a fixed thick gap of 150 μm. The slurry was then dried at room temperature overnight before preparing a set of 10 mm diameter disks. Electrodes were dried at 120 °C overnight under vacuum before being stored in the Glove-Box under argon atmosphere.

2032 coin-type cells were used to assemble Li metal cells for the electrochemical characterization of the negative electrodes. For that, Li was used as the counter electrode (12 nm diameter) and a Whatman separator with 200 μL of 1M $LiPF_6$ in a 50:50 volume mixture of ethylene carbonate (EC) and dimethyl carbonate (DMC) as electrolyte.

The cells were assembled in the Glovebox and then taken out for the electrochemical characterization, which was carried out at laboratory ambient temperature. Cyclic voltammetry (CV) was performed at 0.1 mV s^{-1} scan rate, and in the range from 0.01 to 3.00 V vs Li^+/Li. The EIS measurements were carried out before and after each CV cycle, in frequency range between 300 kHz to 1 Hz. 5 cycles of CV were collected. Galvanostatic Charge Discharge (GCD) measurements were carried out. The galvanostatic cycling protocol used is the following: 10 cycles at 20 mA g^{-1}, 5 cycles at 50 mA g^{-1}, 5 cycles at 100 mA g^{-1}, 5 cycles at 200 mA g^{-1}, 5 cycles at 300 mA g^{-1}, 5 cycles at 500 mA g^{-1}, 5 cycles at 1000 mA g^{-1}, and additional 30 cycles at 20 mA g^{-1}. Moreover, long cycling tests of 200 cycles at 20 mA g^{-1} were performed.

Adhesion characteristics of the lignin-based binder materials were investigated through both manual and mechanical peeling test using a TA.HDplusC Texture Analyser machine with 180º test geometry. The peeling test was carried out at 0.1 m s^{-1} velocity using electrode foil with 5cm x 3cm dimension.

RESULTS AND DISCUSSION

Synthesis and physicochemical properties of carboxymethylated and sulfomethylated Kraft lignin

Kraft lignin was extracted and then modified into carboxymethylated Kraft lignin (CMKL) and sulfomethylated Kraft lignin (SMKL) following the same procedure previously reported. [45]. Briefly, Kraft lignin was precipitated from the industrial black liquor using concentrated H_2SO_4 (96%) dropwise until pH 2. The precipitate was washed with deionized water until neutral pH and dried at 30°C. For the carboxymethylation reaction, lignin was dissolved in 0.15M NaOH solution, and 3 mol of SCA per lignin mol were added. The

modification was carried out at 40°C for 4h, neutralized when finished and purified by dialysis. For the sulfomethylation reaction, lignin was also dissolved in 0.15M NaOH solution and heated to 70°C. 37% formaldehyde and Na_2SO_4 were added afterward, and the temperature was increased to 95°C for 3h, neutralized when finished, and purified by dialysis [45]. For a better understanding of the lignin structure, and the functional groups that take part in both the modification reactions, the overall structure of lignin (a), the lignin alcohols and monolignols from which lignin is derived (b), and the carboxymethylation reaction mechanism (c), and sulfomethylation reaction mechanism (d) are shown in Figure 1.

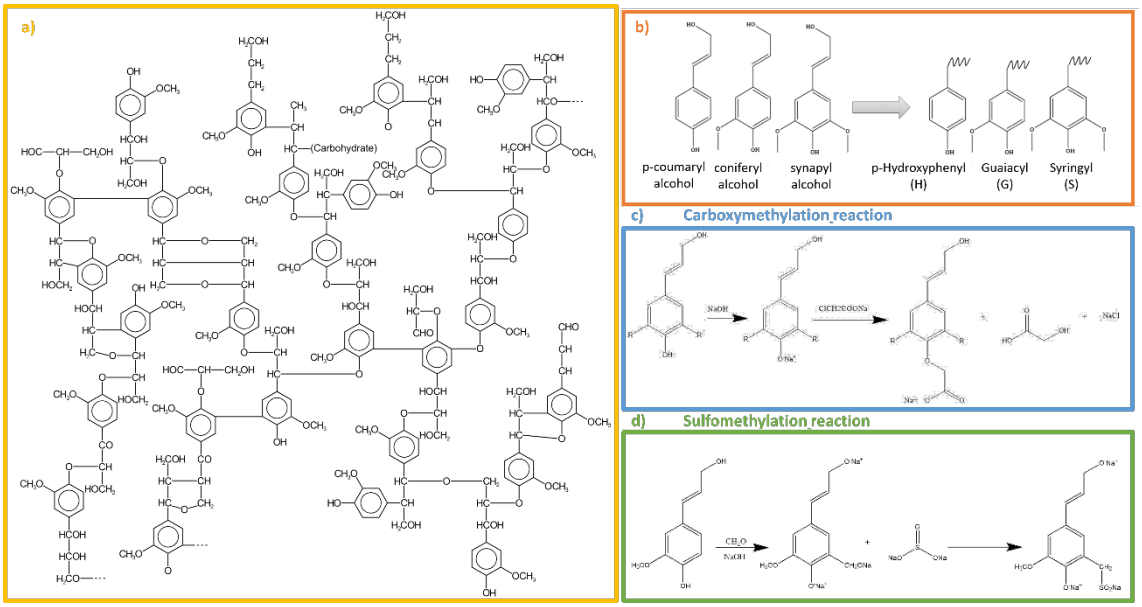


Figure 1. The a) overall lignin structure, b) the lignin alcohols and monolignols from which lignin is derived, c) carboxymethylation reaction, and d) sulfomethylation reaction mechanisms that happen in the alcohol units of the lignin.

As reported in Table S1, the functionalized lignins are characterized by higher values of M_w compared with the standard KL. KL had a M_w of 5048 g/mol that after the carboxymethylation reaction increased to 19154 g/mol, and to 23234 g/mol after the sulfomethylation reaction. This result is an indication of the successful functionalization of Kraft lignin. In addition, the different carbon types identified and quantified by ^{13}C NMR confirmed that the modifications considerably increased the aromatic C-C content, improving the overall aromaticity and conjugated sites in the biopolymer, increasing from 2.78 to 7.14 and 6.10 the aromatic C-C structure abundance due to both the carboxymethylation and sulfomethylation reactions, respectively.

Figure 2 shows the a)FTIR , b) ^{13}C NMR spectra, and c) TGA and DTG curves of KL, CMKL, and SMKL. It can be observed that the functional groups of the lignin varied according to the

chemical reaction carried out. The main functional groups of KL (OH and C=O) reacted with the SCA and Na_2SO_4, causing the decrease of these groups while incrementing condensed structures and carboxymethyl and sulfomethyl groups respectively. ^{13}C NMR verified these results, where a considerable increase in alkyl groups was observed. Additionally, Table S2 shows the different structural moieties calculated and identified from the ^{13}C NMR spectra These results were also reported in another work, where the trend of an increase in the M_w, and higher aromatic and carboxylic content were reported [46].

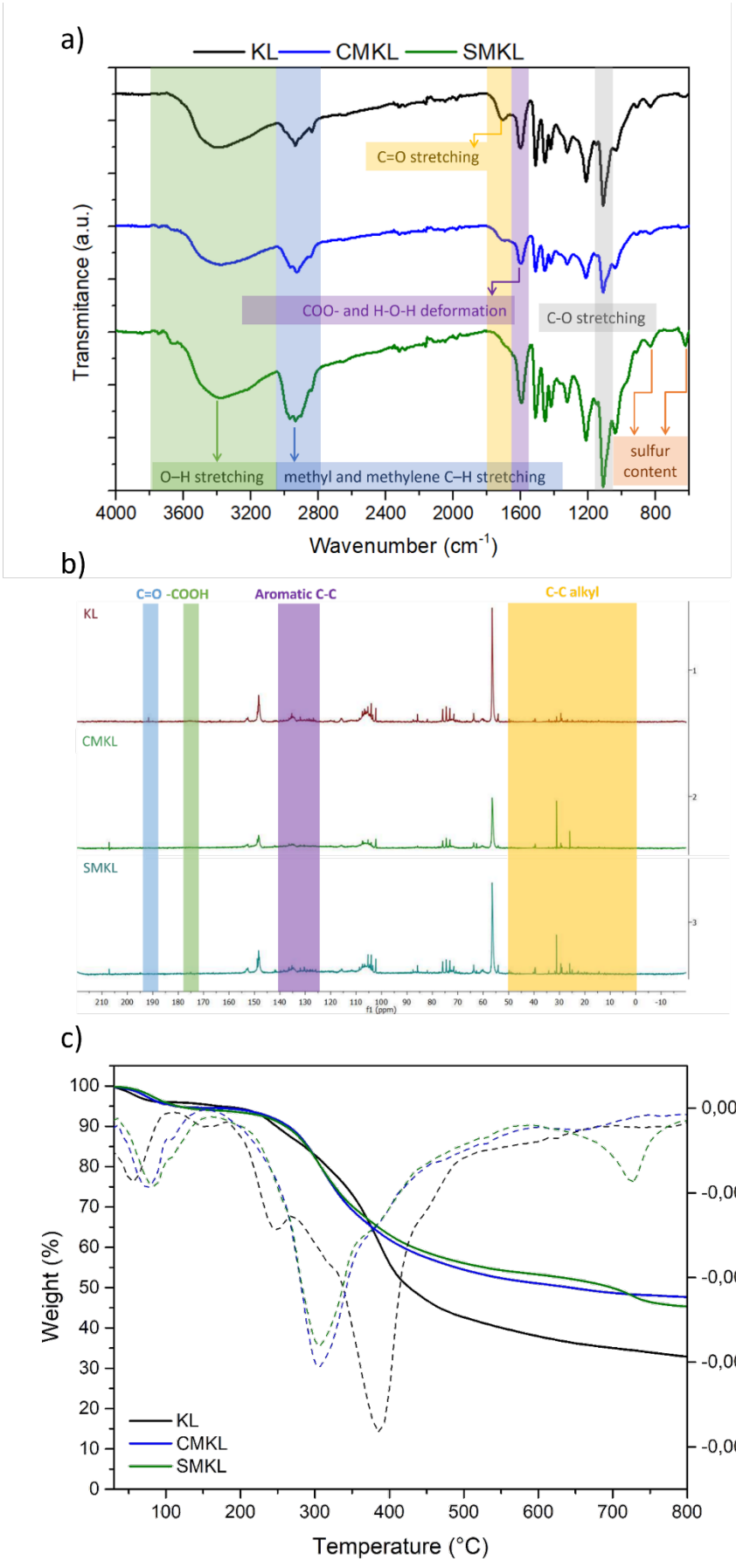


Figure 2. a) FTIR, b)^{13}C NMR, and c) TGA and DTG of KL, CMKL, and SMKL.

TGA and DSC techniques were performed to determine the thermal properties of the KL and its modified analogs. The T_g determination is critical to determine the state in which the polymeric binders work. If the binder material is above its T_g, its rubbery state increases the flexibility of the material, accommodating the volume changes of the electrode during the charging and discharging processes. The ionic conductivity is also higher due to the higher molecular mobility. On the contrary, if it is below, it can cause cracking and loss of adhesion, and the conductivity of the ions is more hindered due to the restricted molecular motion.

The TGA curves and DTG curves shown in Figure 2c indicate the main degradation stages happening during the temperature range. Due to the chemical modifications carried out, the temperature of the main degradation stage decreased from 385 °C to 300 °C in both CMKL and SMKL. Nevertheless, the char residue increased for the modified lignin samples. The KL contained 33% of charred residue, which is in the typical range reported in literature [47], and it increased to 47.5 and 45% in the case of CMKL and SMKL respectively, a phenomenon that commonly happens during chemical modifications of lignin [48]. The T50% was calculated taking into account the char content, which led to values of 375 °C in the case of KL, and 325 °C and 330 °C in the case of CMKL and SMKL. The DSC measurements carried out enabled the calculation of the T_g value, which corresponds to the glass transition temperature. The obtained DSC curves are shown in Figure S1, and T_g values are listed in Table S1. KL shows a T_g value of 134.7 °C, while the modified analogs showed higher values. CMKL had a T_g of 179.2 °C and SMKL had a T_g of 160.0 °C. Although higher T_g values limit the flexibility and ionic mobility, the working conditions of the cell are far below this temperature to see any detrimental effect attributed to the slight increase of the T_g value in the modified lignin particles.

^{31}P NMR spectroscopy was carried out to determine the content of the different hydroxyl groups of the lignin and its modified analogue. For that, the different peaks present in the spectra were identified and integrated, along with the peak corresponding to the internal standard, and the values obtained are shown in Table 2. It can be observed that the sulfomethylation reaction was more efficient on different types of hydroxyl groups present in the lignin, maintaining over 20% of degree of substitution in all the OH types, and reaching almost 50% of substitution in the OH groups of the G units. On the other hand, carboxymethylation did not reach such substitution degrees, with 16.39% of substitution degree for all the OH types, and 21.27% of the total phenolic OH groups. Therefore, it was concluded that that the sulfomethylation reaction conditions were more efficient for the substitution of all the hydroxyl groups present in lignin, while the carboxymethylation reaction was more selective on just substitution the phenolic OH groups.

Table 2. Contents of different hydroxyl groups (mmol/g) quantified by ^{31}P NMR.

	Contents of different hydroxyl groups (mmol OH/g lignin)					TOTAL OH	TOTAL PhOH
	Aliphatic OH	S unit OH	G unit OH	H unit OH	Carboxylic acid OH		
KL	2,20	4,67	0,29	1,51	0,42	9,08	6,46
CMKL	2,17	3,77	0,24	1,08	0,34	7,60	5,09
SMKL	1.71	3.72	0.14	1.15	0.32	7.04	5.01
Degree of substitution (CMKL)	1.75%	19.27%	16.03%	28.45%	18.03%	16.39%	21.27%
Degree of substitution (SMKL)	22.36%	20.33%	49.74%	23.64%	23.98%	22.47%	22.41%

Use of carboxymethylated and sulfomethylated Kraft lignin as aqueous binders for AC electrodes and its electrochemical characterization

To determine if the samples were stable in contact with the electrolyte and able to absorb it, 1g of binder material was submerged in the electrolyte for 1 day. After this time, the binder materials were retrieved, dried, and weighed. It can be observed from Figure S2 and Table S2 that all KL, CMKL, and SMKL samples suffered from solubilization, especially in the case of KL, where after one day the removal of the pellet was almost impossible, while for the case of CMKL and SMKL, the integrity was maintained, and they were able to swell with the electrolyte. 58.35 % of the total KL material submerged in the electrolyte was solubilized, while CMKL and SMKL acquired 12.67% and 5.36% of swelling respectively. Therefore, the carboxymethylation modification largely improved the interaction with the electrolyte. The penetration of the electrolyte in the whole composite electrode is a fundamental parameter that ensures the full utilization of the electrode active material particles. It was observed that the swelling ratio obtained for CMKL was similar to the one reported for CMC in the same working conditions [49].

The adhesive properties of the different lignin-based binders were investigated by peeling test and the force-displacement curves of the CMKL, SMKL and KL electrodes indicate the adhesion between active material, lignin-based binder and Cu. As illustrated in Figure S3, the comparative test allowed to evaluate the adhesive strength of the binders and compactness of the composite material by analyzing the quantity of electrode material removed with the peeling. The visual results are in agreement with data obtained performing the mechanical peeling test with 180º geometry setup. As presented in Figure

S3 CMKL displays the best results with an average peeling force of 1.8 N and a linear behaviour. In contrast, SMKL displays values ranging between 0.8 N and 1.3 N with a less constant profile. Finally, the unmodified KL lignin presented the lower average value of peeling force accompanied by an irregular profile, likely due to the limited binding ability and the poor homogeneity of the composite electrode. Even if the values are slightly lower in comparison with the average ones obtained with modified CMC, which ranges between 3 N and 4 N [50], the improvement of the adhesive properties achieved through the chemical modification of lignin is clearly pointed out.

After a thorough study of the physicochemical and morphological properties of the different lignin samples, their electrochemical performance was investigated. Li metal cells were assembled and tested to explore the Li^+ storage performance and the stability over cycling of the negative electrodes prepared using Kraft lignin or its modified derivatives. The performance of an analogous electrode prepared with CMC as binder is also reported and referred to as benchmark.

Cyclic voltammetry (CV) was used to investigate the behavior of the electroactive species in the electrode. Cells were cycled within the potential range of 0.01-3.00 V vs Li^+/Li at a scan rate of 1 mV s^{-1}. Figure S4 shows the CV curves and Nyquist plots obtained from the EIS measurements for the CMC reference. The intercalation of Li^+ into the anode takes place between 0.3 and 1.5 V [51–53], while the deintercalation process shows a maximum current peak at 0.2 V. The 1st cycle exhibited an irreversible peak between 0.5 and 1 V, which is attributed to the formation of the SEI layer (solid electrolyte interphase) [54]. This results from several irreversible decomposition reactions occurring at the electrode/electrolyte interface involving lithium salts and organic carbonate solvent. The formation of the SEI is crucial for many reasons: it prevents further undesired reactions and degradation by acting as a protective shield, creating a barrier between the electrode and the electrolyte. Indeed, it can enhance the battery stability, performance, and lifespan; but, at the same time, it can also have detrimental effects when the layer becomes too thick or unstable, leading to hindered ion transport and progressive resistance increase [54,55]. Moreover, it has been reported that the binder nature can directly affect the SEI composition, especially when the functional groups that affect the decomposition of the lithium salt are involved [55,56].

Figure 3 displays the CV and Nyquist plots of the unmodified lignin (KL), and the modified lignin samples (CMKL and SMKL). Differently from the CMC, the unmodified KL exhibited two irreversible reduction peaks around 1.2 and 0.7 V vs Li^+/Li during the first scan. On the other side, in the case of CMKL and SMKL, both samples exhibited a single peak at 0.6 V in

the 1st cycle, and another one at 0.85 V during the 2nd cycle, which both disappeared in the 3rd cycle. This behavior can be correlated to a two-step degradation process likely because of the presence of the different functional groups grafted on the KL. Remarkably, the CV profiles of the lignin-based electrode remained stable throughout cycling, without any noticeable losses in the intensity of the redox signals. Despite the comparable behavior observed during CV, the KL-based electrode exhibited slightly higher R_{ct} about 80 Ohm compared with the ones observed using functionalized lignin as binder, which are about 45 Ohm and 40 Ohm for the SMKL and CMKL respectively. The R_{ct} values were extrapolated using the equivalent circuit illustrated in Figure S5, where R1 is assigned to the bulk resistance (R_b) and R2 to the charge-transfer resistance (R_{ct}).

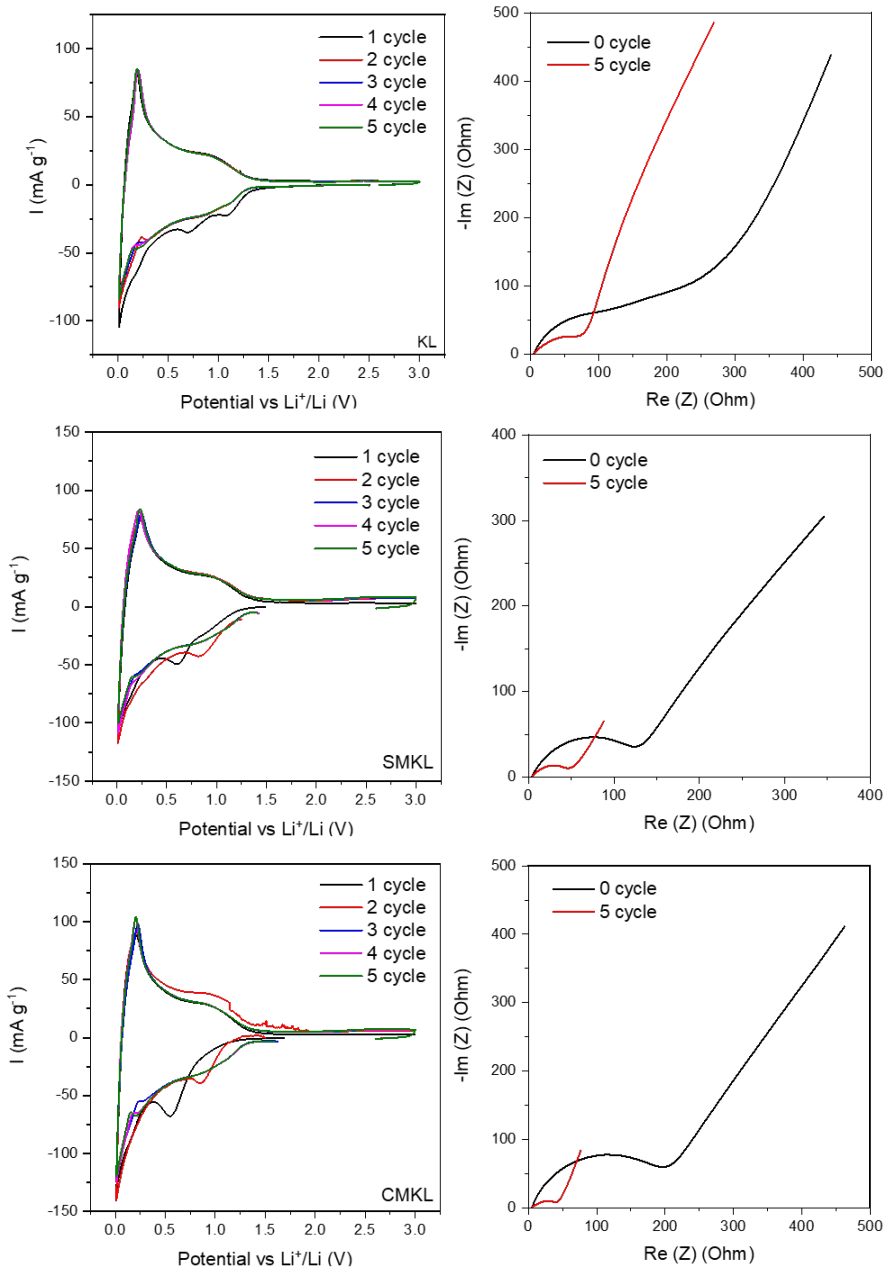


Figure 3. Cyclic voltammetry of KL, CMKL and SMKL (left) with respective Nyquist plot before cycling and after 5 cycles (left).

To further compare the influence of the different bio-based binders on the electrochemical performance of the negative electrodes, galvanostatic cycling was performed at different current densities at 25 °C as described in the method section. Charge and discharge profiles and specific capacity values vs cycles are reported in Figure 4. CMC-based electrode delivered good specific capacity, with values of 200 mA h g^{-1} at the lowest specific current (20 mA g^{-1}), which gradually decreased following the current increase up to 120 mA h g^{-1} at 1000 mA g^{-1}. During the cycling at 20 mA g^{-1} the cell delivered stable specific capacity values about 215 mA h g^{-1}. In contrast, the electrode based on the KL binder showed lower capacity

values, specifically 125 mA h g^{-1} and 65 mA h g^{-1}, at 20 mA g^{-1} and 1000 mA g^{-1}, respectively. Noteworthy, the carboxymethylation and sulfomethylation modifications allowed to obtain higher specific capacity outputs, especially in the case of CMKL. In detail, the Li metal cell based on CMKL delivered 175 mA h g^{-1} at 20 mA g^{-1} and more than 100 mA h g^{-1} at the highest current density of 1000 mA g^{-1}. On the other side, the sample SMKL exhibited slightly lower values with the maximum value of 140 mA h g^{-1} at 20 mA g^{-1}.

The voltage vs specific capacity plot for all samples presented well defined insertion and de-insertion process in/from negative electrodes occurring below 1V vs Li^+/Li without any signs of side reactions or strong polarization, even at relatively high current densities such as 1000 mA g^{-1}. Furthermore, CMKL sample showed a lower voltage drop in comparison with KL and SMKL samples, suggesting a more efficient and less resistive Li^+ cation insertion/de-insertion mechanism, likely due to the formation of a more conductive and thinner SEI and a better active material particles distribution and cohesion.

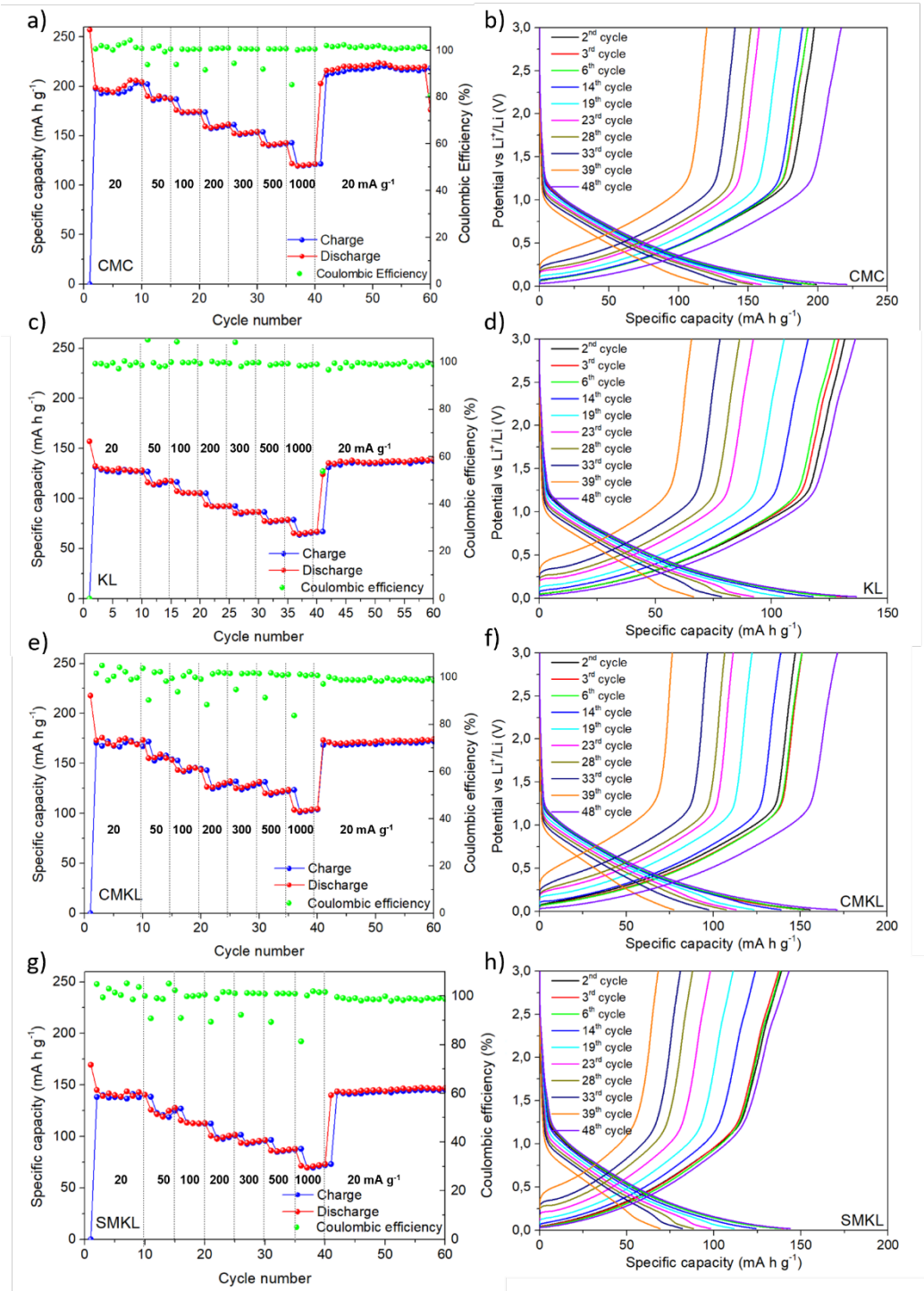


Figure 4. GCD cycling (left) and charge/discharge profiles (right) of the anodes prepared with different binders (CMC, KL, CMKL, SMKL).

Figure 5 shows the long cycling results of the anodic electrodes formulated using CMC, KL, CMKL, and SMKL as binder materials. All samples showed similar capacity values, maintaining a stable cycling throughout the 200 cycles recorded. CMKL showed the best result between the lignin samples, validating its resemblance to the commercially used CMC, which showed slightly better capacity values. KL and SMKL were similar to each other, with

somewhat lower capacity values than the CMKL, concluding once again that the carboxymethylation reaction was the optimal option of modification for lignin for this application.

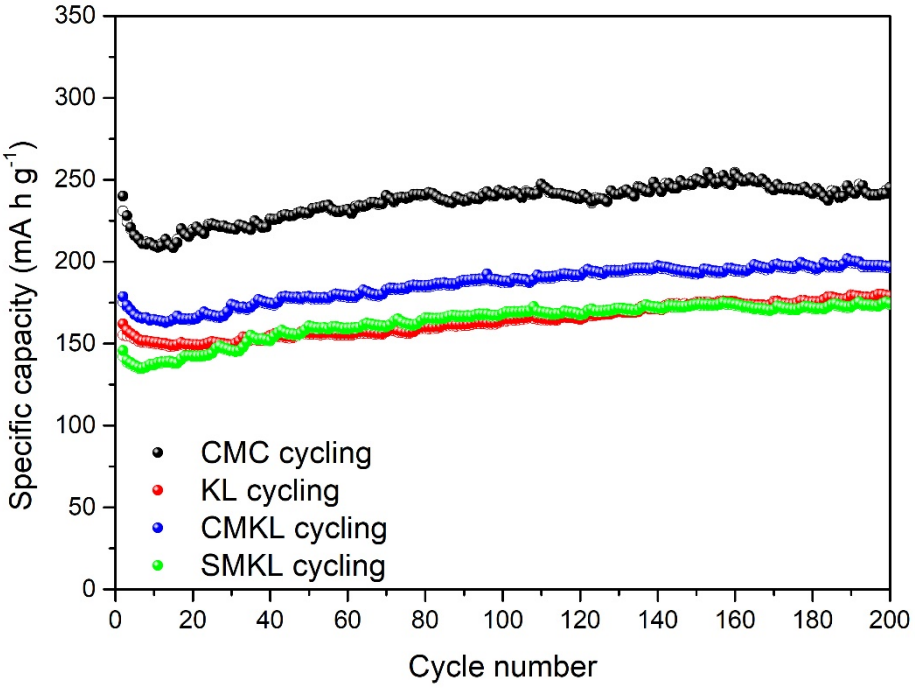


Figure 5. Long cycling comparison at 20 mA g^{-1} of the anodes formulated with CMC, KL, CMKL, and SMKL as binder.

CONCLUSIONS

The findings of this study indicated that the synthesized lignin products are suitable materials to incorporate as binder materials in the formulation of negative electrodes for Lithium batteries. This breakthrough opens promising opportunities to valorize this complex biomaterial derived from wood, traditionally considered a waste, repurposing it as a viable substitute for the currently employed synthetic binder materials for electrodes. Noteworthy, the carboxymethylated Kraft lignin showed promising performance as a binder material with CMKL-based cell delivering 175 mA h g^{-1} at 20 mA g^{-1} and more than 100 mA h g^{-1} at the highest current density of 1000 mA g^{-1}. In addition the CMKL sample exhibited superior capacity output during the long cycling in comparison with the SMKL and KL samples. This work demonstrates for the first time the potential to utilize carboxymethylated lignin in similar ways as the commercially employed CMC, with still room for some improvements like a higher substitution rate in the chemical modification that would therefore improve the integrity and electrochemical properties of the electrodes,

increasing their compatibility with the typical organic solvent-based electrolytes and improving the adhesion onto the current collector. Moreover, the implementation of this product not only addresses environmental concerns associated with waste management but also contributes to the development of more sustainable and eco-friendly energy storage technologies.

ACKNOWLEDGEMENTS

The authors would like to acknowledge the financial support of the Basque Government through the grant PIF19-183 and project IT1498-22. G. Lingua acknowledges the funding from the European Union's Horizon 2020 research and innovation programme under the Marie Skłodowska-Curie grant agreement No 101034379.

References

[1] Hannan MA, Wali SB, Ker PJ, Rahman MSA, Mansor M, Ramachandaramurthy VK, et al. Battery energy-storage system: A review of technologies, optimization objectives, constraints, approaches, and outstanding issues. J Energy Storage 2021;42:103023. https://doi.org/10.1016/J.EST.2021.103023.

[2] Zhou J, Qian T, Yang T, Wang M, Guo J, Yan C. Nanomeshes of highly crystalline nitrogen-doped carbon encapsulated Fe/Fe3C electrodes as ultrafast and stable anodes for Li-ion batteries. J Mater Chem A 2015;3:15008–14. https://doi.org/10.1039/c5ta03312h.

[3] Wang Y, Liu J, Ji H, Wang S, Wang M, Zhou X, et al. Optimizing Si–O Conjugation to Enhance Interfacial Kinetics for Low-Temperature Rechargeable Lithium-Ion Batteries. Adv Mater 2024;2:1–10. https://doi.org/10.1002/adma.202412155.

[4] Xu N, Ma X, Wang M, Qian T, Liang J, Yang W, et al. Stationary Full Li-Ion Batteries with Interlayer-Expanded V6O13 Cathodes and Lithiated Graphite Anodes. Electrochim Acta 2016;203:171–7. https://doi.org/10.1016/j.electacta.2016.04.044.

[5] Dobryden I, Montanari C, Bhattacharjya D, Aydin J, Ahniyaz A. Bio-Based Binder Development for Lithium-Ion Batteries. Materials (Basel) 2023;16. https://doi.org/10.3390/ma16165553.

[6] Wang F, Ouyang D, Zhou Z, Page SJ, Liu D, Zhao X. Lignocellulosic biomass as sustainable feedstock and materials for power generation and energy storage. J Energy Chem 2021;57:247–80. https://doi.org/10.1016/j.jechem.2020.08.060.

[7] Yu O, Kim KH. Lignin to materials: A focused review on recent novel lignin applications. Appl Sci 2020;10. https://doi.org/10.3390/app10134626.

[8] Naseem A, Tabasum S, Mahmood K, Zuber M, Ali M, Noreen A. Lignin-derivatives based polymers , blends and composites : A review. Int J Biol Macromol 2016;93:296–313. https://doi.org/10.1016/j.ijbiomac.2016.08.030.

[9] Liu H, Xu T, Liu K, Zhang M, Liu W, Li H, et al. Lignin-based electrodes for energy storage application. Ind Crops Prod 2021;165. https://doi.org/10.1016/j.indcrop.2021.113425.

[10] Sternberg J, Sequerth O, Pilla S. Green chemistry design in polymers derived from lignin: review and perspective. Prog Polym Sci 2021;113. https://doi.org/10.1016/j.progpolymsci.2020.101344.

[11] Li JT, Wu ZY, Lu YQ, Zhou Y, Huang Q Sen, Huang L, et al. Water Soluble Binder, an Electrochemical Performance Booster for Electrode Materials with High Energy Density. Adv Energy Mater 2017;7:1–30. https://doi.org/10.1002/aenm.201701185.

[12] Luo L, Xu Y, Zhang H, Han X, Dong H, Xu X, et al. Comprehensive Understanding of High Polar Polyacrylonitrile as an Effective Binder for Li-Ion Battery Nano-Si Anodes. ACS Appl Mater Interfaces 2016;8:8154–61. https://doi.org/10.1021/acsami.6b03046.

[13] Costa CM, Silva MM, Lanceros-Méndez S. Battery separators based on vinylidene fluoride (VDF) polymers and copolymers for lithium ion battery applications. RSC Adv 2013;3:11404–17. https://doi.org/10.1039/c3ra40732b.

[14] Wang R, Feng L, Yang W, Zhang Y, Zhang Y, Bai W, et al. Effect of Different Binders on the Electrochemical Performance of Metal Oxide Anode for Lithium-Ion Batteries. Nanoscale Res Lett 2017;12. https://doi.org/10.1186/s11671-017-2348-6.

[15] Qiu L, Shao Z, Wang D, Wang F, Wang W, Wang J. Novel polymer Li-ion binder carboxymethyl cellulose derivative enhanced electrochemical performance for Li-ion batteries. Carbohydr Polym 2014;112:532–8. https://doi.org/10.1016/j.carbpol.2014.06.034.

[16] Wang H, Yang Y, Gao C, Chen T, Song J, Zuo Y, et al. An entanglement association polymer electrolyte for Li-metal batteries. Nat Commun 2024;15:1–12. https://doi.org/10.1038/s41467-024-46883-8.

[17] Díaz-Ramírez MC, Ferreira VJ, García-Armingol T, López-Sabirón AM, Ferreira G. Environmental Assessment of Electrochemical Energy Storage Device Manufacturing to Identify Drivers for Attaining Goals of Sustainable Materials 4.0. Sustainability 2020;12.

[18] Mun SC, Jeon YH, Won JH. Progress and challenges for replacing n-methyl-2-pyrrolidone / polyvinylidene fluoride slurry formulations in lithium-ion battery cathodes. Prog Nat Sci Mater Int 2024;34:194–206. https://doi.org/10.1016/j.pnsc.2024.02.013.

[19] Dhanalekshmi KI, Magesan P, Ma X, Zhang X, Jayamoorthy K. Sustainable development of anode materials for non-aqueous potassium ion batteries. J Energy Storage 2023;68:107691. https://doi.org/10.1016/j.est.2023.107691.

[20] Liu G, Zhao Z, Ghahreman A. Hydrometallurgy Novel approaches for lithium extraction from salt-lake brines : A review. Hydrometallurgy 2019;187:81–100. https://doi.org/10.1016/j.hydromet.2019.05.005.

[21] Smink D, Kersten SRA, Schuur B. Separation and Puri fi cation Technology Recovery of lignin from deep eutectic solvents by liquid-liquid extraction. Sep Purif Technol 2020;235:116127. https://doi.org/10.1016/j.seppur.2019.116127.

[22] Vandepaer L, Cloutier J, Amor B. Environmental impacts of Lithium Metal Polymer and Lithium-ion stationary batteries. Renew Sustain Energy Rev 2017;78:46–60. https://doi.org/10.1016/j.rser.2017.04.057.

[23] Gu X, Ieromonachou P, Zhou L, Tseng M. Developing pricing strategy to optimise total pro fi ts in an electric vehicle battery closed loop supply chain. J Clean Prod

2018;203:376–85. https://doi.org/10.1016/j.jclepro.2018.08.209.

[24] Ishii M, Makino S, Nakamura H. The role of carboxymethyl cellulose on the rheology of anode slurries in lithium-ion batteries. Curr Opin Colloid Interface Sci 2024;74:101858. https://doi.org/10.1016/j.cocis.2024.101858.

[25] Erdoğan O, Sendogdular ST. Wettability and plasticizing effect of CO2 on Si/C electrode in lithium-ion batteries. J Polym Res 2024;31:1–10. https://doi.org/10.1007/s10965-024-04052-x.

[26] Jin C, Nai J, Sheng O, Yuan H, Zhang W, Tao X, et al. Biomass-based materials for green lithium secondary batteries. Energy Environ Sci 2021;14:1326–79. https://doi.org/10.1039/d0ee02848g.

[27] Bresser D, Buchholz D, Moretti A, Passerini S, Varzi A, Buchholz D. Alternative binders for sustainable electrochemical energy storage – the transition bio-derived polymers. Energy Environ Sci 2018;11:3096. https://doi.org/10.1039/c8ee00640g.

[28] Buqa H, Holzapfel M, Krumeich F, Veit C, Nov P. Study of styrene butadiene rubber and sodium methyl cellulose as binder for negative electrodes in lithium-ion batteries 2006;161:617–22. https://doi.org/10.1016/j.jpowsour.2006.03.073.

[29] Gordon R. Effect of carboxymethyl cellulose on the flow behavior of lithium-ion battery anode slurries and the electrical as well as mechanical properties of corresponding dry layers. J Mater Sci 2020;55:15867–81. https://doi.org/10.1007/s10853-020-05122-3.

[30] Versaci D, Nasi R, Zubair U, Amici J, Sgroi M, Dumitrescu MA. New eco-friendly low-cost binders for Li-ion anodes 2019:3429–35. https://doi.org/10.1007/s10008-017-3665-5.

[31] Mecerreyes D, Casado N, Villaluenga I, Forsyth M. Current Trends and Perspectives of Polymers in Batteries. Macromolecules 2024;57:3013–25. https://doi.org/10.1021/acs.macromol.3c01971.

[32] Rolandi AC, Pozo-Gonzalo C, de Meatza I, Casado N, Forsyth M, Mecerreyes D. Carrageenans as Sustainable Water-Processable Binders for High-Voltage NMC811 Cathodes. ACS Appl Energy Mater 2023;6:8616–25. https://doi.org/10.1021/acsaem.3c01662.

[33] Rolandi AC, Barquero A, Pozo-Gonzalo C, de Meatza I, Casado N, Forsyth M, et al. Biobased Acrylic Latexes/Sodium Carboxymethyl Cellulose Aqueous Binders for Lithium-Ion NMC 811 Cathodes. ACS Appl Polym Mater 2024;6:1236–44. https://doi.org/10.1021/acsapm.3c02167.

[34] Boerjan W, Ralph J, Baucher M. Lignin Biosynthesis. Annu Rev Plant Biol 2003;54:519–46. https://doi.org/10.1146/annurev.arplant.54.031902.134938.

[35] Balakshin MY, Capanema EA, Sulaeva I, Schlee P, Huang Z, Feng M, et al. New Opportunities in the Valorization of Technical Lignins. ChemSusChem 2021;14:1016–36. https://doi.org/10.1002/cssc.202002553.

[36] Li T, Takkellapati S. The current and emerging sources of technical lignins and their applications. Biofuels, Bioprod Biorefining 2018;12:756–87. https://doi.org/10.1002/BBB.1913.

[37] Fatehi P, Ni Y. Integrated forest biorefinery - Sulfite process. ACS Symp Ser

2011;1067:409–41. https://doi.org/10.1021/bk-2011-1067.ch016.

[38] Dessbesell L, Paleologou M, Leitch M, Pulkki R, Xu C (Charles). Global lignin supply overview and kraft lignin potential as an alternative for petroleum-based polymers. Renew Sustain Energy Rev 2020;123:109768. https://doi.org/10.1016/j.rser.2020.109768.

[39] Xie ZH, Zhou JH, Li HM, Sun GW. Comparison between Green Liquor Pretreatment-Kraft Pulping and Conventional Kraft Pulping. Adv Mater Res 2013;781–784:2650–3. https://doi.org/10.4028/WWW.SCIENTIFIC.NET/AMR.781-784.2650.

[40] Zevallos Torres LA, Lorenci Woiciechowski A, de Andrade Tanobe VO, Karp SG, Guimarães Lorenci LC, Faulds C, et al. Lignin as a potential source of high-added value compounds: A review. J Clean Prod 2020;263. https://doi.org/10.1016/j.jclepro.2020.121499.

[41] Lu H, Cornell A, Alvarado F, Behm M, Leijonmarck S, Li J, et al. Lignin as a binder material for eco-friendly Li-ion batteries. Materials (Basel) 2016;9:1–17. https://doi.org/10.3390/ma9030127.

[42] Chen T, Zhang Q, Pan J, Xu J, Liu Y, Al-Shroofy M, et al. Low-Temperature Treated Lignin as Both Binder and Conductive Additive for Silicon Nanoparticle Composite Electrodes in Lithium-Ion Batteries. ACS Appl Mater Interfaces 2016;8:32341–8. https://doi.org/10.1021/acsami.6b11500.

[43] Chen Z, Lu M, Qian Y, Yang Y, Liu J, Lin Z, et al. Ultra-Low Dosage Lignin Binder for Practical Lithium–Sulfur Batteries. Adv Energy Mater 2023;13:2300092. https://doi.org/https://doi.org/10.1002/aenm.202300092.

[44] Nirmale TC, Kale BB, Varma AJ. A review on cellulose and lignin based binders and electrodes: Small steps towards a sustainable lithium ion battery. Int J Biol Macromol 2017;103:1032–43. https://doi.org/10.1016/j.ijbiomac.2017.05.155.

[45] Izaguirre N, Erdocia X, Labidi J. Exploring chemical reactions to enhance thermal and dispersion stability of kraft and organosolv lignin. Int J Biol Macromol 2024;264:130518. https://doi.org/10.1016/j.ijbiomac.2024.130518.

[46] Chen K, Lei L, Lou H, Niu J, Yang D, Qiu X, et al. High internal phase emulsions stabilized with carboxymethylated lignin for encapsulation and protection of environmental sensitive natural extract. Int J Biol Macromol 2020;158:430–42. https://doi.org/10.1016/j.ijbiomac.2020.04.106.

[47] Chollet B, Lopez-Cuesta JM, Laoutid F, Ferry L. Lignin nanoparticles as a promising way for enhancing lignin flame retardant effect in polylactide. Materials (Basel) 2019;12. https://doi.org/10.3390/ma12132132.

[48] Sameni J, Krigstin S, Rosa D dos S, Leao A, Sain M. Thermal characteristics of lignin residue from industrial processes. BioResources 2014;9:725–37. https://doi.org/10.15376/biores.9.1.725-737.

[49] Zhang Z, Zeng T, Lai Y, Jia M, Li J. A comparative study of different binders and their effects on electrochemical properties of LiMn2O4 cathode in lithium ion batteries. J Power Sources 2014;247:1–8. https://doi.org/10.1016/j.jpowsour.2013.08.051.

[50] Jiang HW, Yang Y, Nie YM, Su ZF, Long YF, Wen YX, et al. Cross-linked β-CD-CMC as an

effective aqueous binder for silicon-based anodes in rechargeable lithium-ion batteries. RSC Adv 2022;12:5997–6006. https://doi.org/10.1039/d1ra08538g.

[51] Yang G, Li X, Guan Z, Tong Y, Xu B, Wang X, et al. Insights into lithium and sodium storage in porous carbon. Nano Lett 2020;20:3836–43. https://doi.org/10.1021/acs.nanolett.0c00943.

[52] Huang Y, Wang Y, Bai P, Xu Y. Storage Mechanism of Alkali Metal Ions in the Hard Carbon Anode: An Electrochemical Viewpoint. ACS Appl Mater Interfaces 2021;13:38441–9. https://doi.org/10.1021/acsami.1c12150.

[53] Xie L, Tang C, Bi Z, Song M, Fan Y, Yan C, et al. Hard Carbon Anodes for Next-Generation Li-Ion Batteries: Review and Perspective. Adv Energy Mater 2021;11:1–22. https://doi.org/10.1002/aenm.202101650.

[54] Song W, Scholtis S, Sherrell PC, Tsang DKH, Ngiam J, Lischner J, et al. Electronic structure influences on the formation of the solid electrolyte interphase. Energy Environ Sci 2020;13:4977–89. https://doi.org/10.1039/d0ee01825b.

[55] Young BT, Nguyen CC, Lobach A, Heskett DR, Woicik JC, Lucht BL. Role of binders in solid electrolyte interphase formation in lithium ion batteries studied with hard X-ray photoelectron spectroscopy. Jouranl Mater Res 2019;34:97–106. https://doi.org/10.1557/jmr.2018.363.

[56] Johnson R, Waller GH, Bezsonov I, Mansour AN, Nadimpalli SPV. Impact of Binder Thin-Films on Surface Chemistry of Silicon Anodes in Lithium-Ion Batteries. ECS Adv 2024;3. https://doi.org/10.1149/2754-2734/ad69a5.